ORIGINAL

Supercritical CO_2 drying of New Zealand red beech to below the fibre saturation point reduces collapse distortion

Hamish Pearson[1] · Lloyd Donaldson[1] · Mark Kimberley[2] · Bruce Davy[1]

Abstract

Supercritical CO_2 offers an alternative method of removing wood moisture and reducing cellular collapse compared to traditional drying techniques. The technique has been previously demonstrated for *Pinus radiata* and *Eucalyptus nitens* dewatering and was modified in this study for New Zealand red beech (*Nothofagus fusca*) heartwood, which is notoriously difficult to dry without causing excessive distortion. The technique was also successfully extended to drying below the fibre saturation point. A specific dewatering and drying schedule was developed for *N. fusca* because of negligible dewatering using a schedule previously designed for wood with an open hydrofluidic network of interconnected vessels. An anatomical assessment confirmed lumen pathways were occluded with tyloses and polyphenol resins. A fluid dynamics assessment concluded that permeability measurements are recommended together with tortuosity and porosity information for improved wood species dewatering characterisation. Using the dewatering and drying schedule, collapse was successfully reduced by 92% for both normalised internal wood area and void collapse when compared to oven-dried samples. The beech specimens took 18 days to reach 17.3% moisture content (MC) but displayed some checking from early dewatering depressurisation, compared to air-dried control specimens which showed no collapse or checking but took 6 months to reach 12% MC. Supercritical CO_2 dewatering and drying could be combined with extractives separation, preservative treatment, and mechanical forming of wood in one plant to make a potentially economically viable process with improved energy, environmental and carbon footprints. A techno-economic analysis is suggested to fully compare supercritical drying of wood against conventional drying operations.

✉ Hamish Pearson
  Hamish.Pearson@scionresearch.com

1   Scion. 49 Sala Street, Private Bag 3020, Rotorua, New Zealand

2   72 Becroft Drive, Forrest Hill, Auckland 0620, New Zealand

Introduction

Supercritical CO_2 dewatering followed by oven-drying has previously been shown to reduce collapse in *Eucalyptus nitens* ((H. Deane & Maiden) Maiden) wood by over 90% using a novel 4-h dewatering treatment schedule (Pearson et al. 2022). Testing the same technology on New Zealand's indigenous red beech timber (*Nothofagus fusca* ((Hook. F.) Oerst.)) allows the process to be tested at the extreme. This is because *N. fusca* is notoriously difficult to dry without causing unwanted collapse and related distortion (Reid 1953; Clifton 1990), and is among the most refractory timbers to be dried in the world (Zhang 2000). Out of the five main New Zealand *Nothofagus* species, only hard beech (*N. truncata* ((Col.) Ckn.)) yields a similar level of distortion but takes less time to conventionally dry (Kininmonth 1964). Therefore *N. fusca* is an ideal proxy species for difficult-to-dry woods worldwide.

Nothofagus fusca has many appealing qualities such as texture, colour, durability, hardness and strength (Haslett and Kininmonth 1986; Clifton 1990; Smale et al. 2012). Once dried to a suitable equilibrium moisture content (MC) it has been reported as having exceptional dimensional stability, compared to all other New Zealand timber species, by being resistant to further fluctuations in atmospheric humidity (Orman and Harris 1964; Wardle 1984). Previous methods for drying *N. fusca* have focussed on singular operations, or combinations of: air-drying, kiln-drying, pre-drying, steam reconditioning, hot water soaking, dehumidification, and oscillatory or intermittent (stepwise) drying (Kininmonth 1971, 1972; Haslett and Kininmonth 1986; Clifton 1990; Langrish et al. 1992; Zhang 2000; Herritsch et al. 2010; Herritsch and Nijdam 2012). However, mild air-drying of 25 mm thick boards to 12% MC typically requires 10–12 months with collapse being prevalent and unable to be dressed out (Kininmonth 1964). Even kiln schedules designed for difficult-to-dry *Eucalyptus* species such as ironbark (*E. indurata* (Brooker & Hopper)) have been unsuccessful when applied to *N. fusca*, which reveals how difficult the species is to dry (Zhang 2000).

The slow drying rate and collapse during drying of *N. fusca* may be due to the presence of extensive encrustations of polyphenolic extractives which occlude the cell lumina and pit membranes in heartwood (Hillis and Orman 1962; Hillis and Inoue 1967; Kininmonth 1971; Lloyd 1976; Haslett and Kininmonth 1986). Excessive collapse and distortion have also been attributed to the presence of tension wood which can be only partially recovered with steam reconditioning (Kininmonth 1964; Washusen and Ilic 2001; Chauhan and Walker 2011). *N. fusca* typically has narrow sized vessels and exhibits the greatest proportion of heartwood with the highest levels of heartwood extractives, at around 10% by weight, compared to the rest of the New Zealand beeches (Orman and Harris 1964; Purnell 1964).

Supercritical CO_2 has previously been widely used for the separation of extractives (Williams et al. 2002; Kopcak and Mohamed 2005; Herrero et al. 2006; Bulushi et al. 2018), food drying (Brown et al. 2008; Khalloufi et al. 2010) and wood treatments (Kaye et al. 1999; Hay and Johns 2000; Stahl and Bentz

2004; Oberdorfer et al. 2006; Kjellow and Henriksen 2009; Matsunaga et al. 2010; Gething 2011; Fernandes et al. 2012; Gething et al. 2013; Gabitov et al. 2017; Aggarwal et al. 2019; Zhang et al. 2021). However, it also offers a unique method for minimising distortion in solid wood during dewatering (Jones and Walker 1999; Kaye et al. 1999; Blakemore and Northway 2009; Franich et al. 2014; Asafu-Adjaye et al. 2021; Zhang et al. 2021; Liu et al. 2022; Pearson et al. 2022) and drying compared to conventional timber drying methods. Conventional drying kilns typically require less capital expenditure but involve greater running costs because of the thermal energy and time required to evaporate moisture. Kilns also typically emit volatiles into the atmosphere as a by-product. By comparison, supercritical CO_2 dewatering offers a faster and less energy intensive moisture removal system because it is a physicochemical process. Not only can CO_2 be recycled, but all emissions can be captured as extractives. Moreover, dewatering could theoretically also be extended to drying below the fibre saturation point (FSP) by utilising the moisture absorption capability of CO_2 (Sabirzyanov et al. 2002), which is a process that has not been previously reported for wood drying. The technology is capital intensive but could combine several unit operations such as dewatering, drying, extractives separation, preservative treatment and mechanical forming of wood in one plant to make a potentially economically viable process with an improved environmental footprint (Pearson et al. 2022).

The objectives of this study were firstly to test the robustness of supercritical CO_2 dewatering of *N. fusca* by characterising its wood anatomy and hydrofluidic characteristics. Secondly, the dewatering efficacy of *N. fusca* was compared with previously developed schedules for *Pinus radiata* (D. Don) and *E. nitens* using a suitable dewatering and drying schedule for beech based upon the dewatering and anatomy results. Finally, by comparing relative collapse between treatments, the feasibility of reducing collapse in *N. fusca* using supercritical CO_2 was assessed.

Materials and methods

Specimen preparation

Nothofagus fusca was sourced from a natural stand at Maruia (lat. 42°11.3'S, long. 172°13.6'E) in the West Coast region of the South Island of New Zealand. Six trees were randomly selected, sawn at a height of 1800 mm above the ground, and helicopter logged to the nearby Forever Beech Ltd sawmill at Reefton. Six clear-wood boards, each measuring 80 mm×30 mm (*rad-tan* face)×1500 mm (*long* direction) were immediately removed from the outer layer of heartwood of the base of each log before being end sealed with wax, wrapped in plastic, and transported under refrigerated conditions to Scion, Rotorua, New Zealand. Eight specimens measuring 25 mm×25 mm (*rad-tan* face)×200 mm (*long* direction) were removed from one randomly selected board from each log and labelled as shown in Fig. 1. One test specimen measuring 70 mm×30 mm (*rad-tan* face)×50 mm (*long* direction) was also cross-cut from the middle of each selected board for microscopy assessment. All 48, 25 mm square by
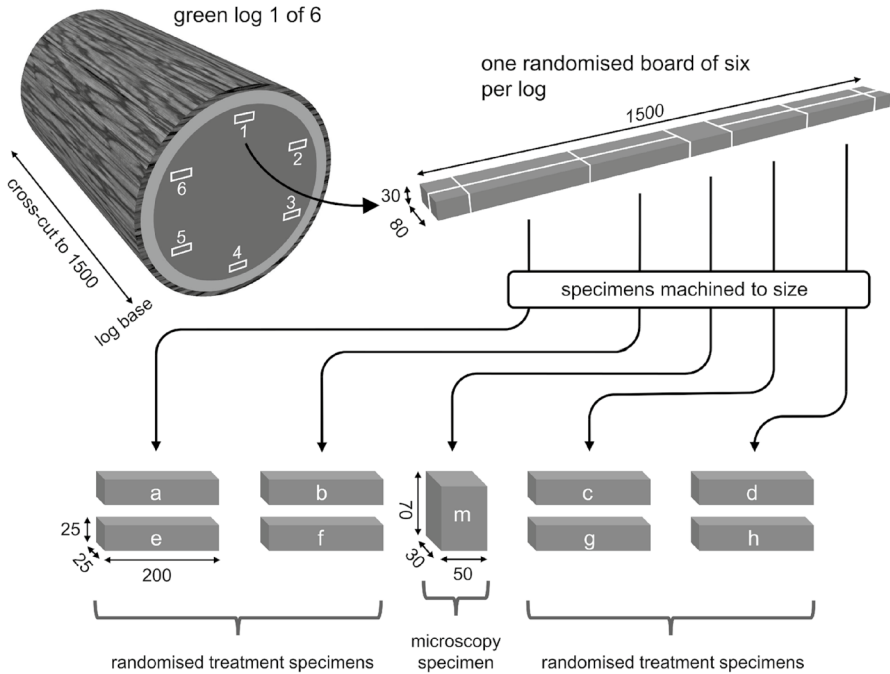
Fig. 1 Beech specimen preparation scheme where dimensions are in mm. The 'a' and 'e' specimens relate to wood removed from the base end of each log

200 mm long specimens were then randomised for treatments. Each specimen was wrapped in plastic and refrigerated at 4 °C before being dimensionally measured and weighed prior to treatment. Eighteen specimens (3 per tree) were used in the three dewatering treatments, 6 specimens (1 per tree) were oven-dried, 6 specimens (1 per tree) were air-dried, and 6 specimens (1 per tree) used to estimate free-shrinkage. This left 2 back-up specimens per tree which were not required for the study. Depending on the timing of treatments, green MC and basic density was measured for each specimen using the water displacement method (ASTM 2014c) and specimens were oven-dried at 103 °C for density, MC and collapse measurements (ASTM 2014b).

Wood anatomy assessment

Cell dimensions including vessel and fibre lumen area and diameter, and cell wall thickness, were measured by image analysis of transverse sections using Digital Optics V + +. Wood sections from each of the 6 microscopy specimens were stained in aqueous safranin for 10 min and washed in water followed by air-drying under restraint by clamping sections between 2 microscope slides to prevent curling. Dry sections were transferred to xylene and mounted in EUKITT before imaging. Samples were also screened for the presence of gelatinous fibres and tyloses in vessels. Images to illustrate wood anatomy were acquired using confocal fluorescence

microscopy of wood autofluorescence from lignin and extractives. Excitation was 488 nm and emission was 500–550 nm and images were rendered as maximum intensity projections or as single optical slices.

Supercritical CO_2 dewatering apparatus

Supercritical CO_2 dewatering relates to a method to reduce lumen water, also known generally as 'free-water' (Thybring and Fredriksson 2023), from wood cells. The method utilises the physicochemical behaviour of CO_2 when dissolved CO_2 creates gaseous back-pressure to force lumen moisture from the open hydrofluidic network of wood xylem upon pressure release (Dawson et al. 2015). Supercritical CO_2 beech dewatering was performed in a previously developed 0.5 L treatment plant (Fig. 2) that was designed to operate at pressures from atmospheric to 30 MPa and temperatures up to 90 °C (Dawson et al. 2015; Pearson et al. 2019b). The plant was calibrated and able to control pressure and temperature setpoints to similar values to those reported earlier (Pearson et al. 2019a).
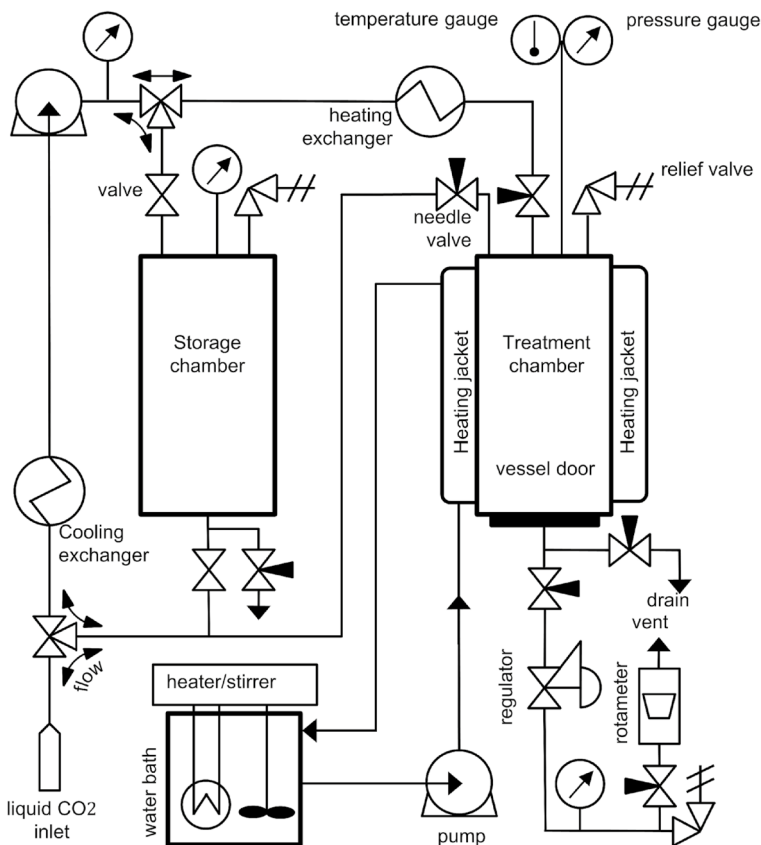
Fig. 2 Schematic of supercritical CO_2 dewatering plant

Dewatering involved treating beech with one of three treatment schedules by manipulating pressure as a function of time as shown in Fig. 3. Each schedule

Fig. 3 Graphical representation of dewatering/drying schedules used for beech experimentation showing pressure manipulation as a function of time. **a** 'radiata' dewatering schedule, **b** 'nitens' dewatering schedule, **c** 'beech' dewatering and drying schedule
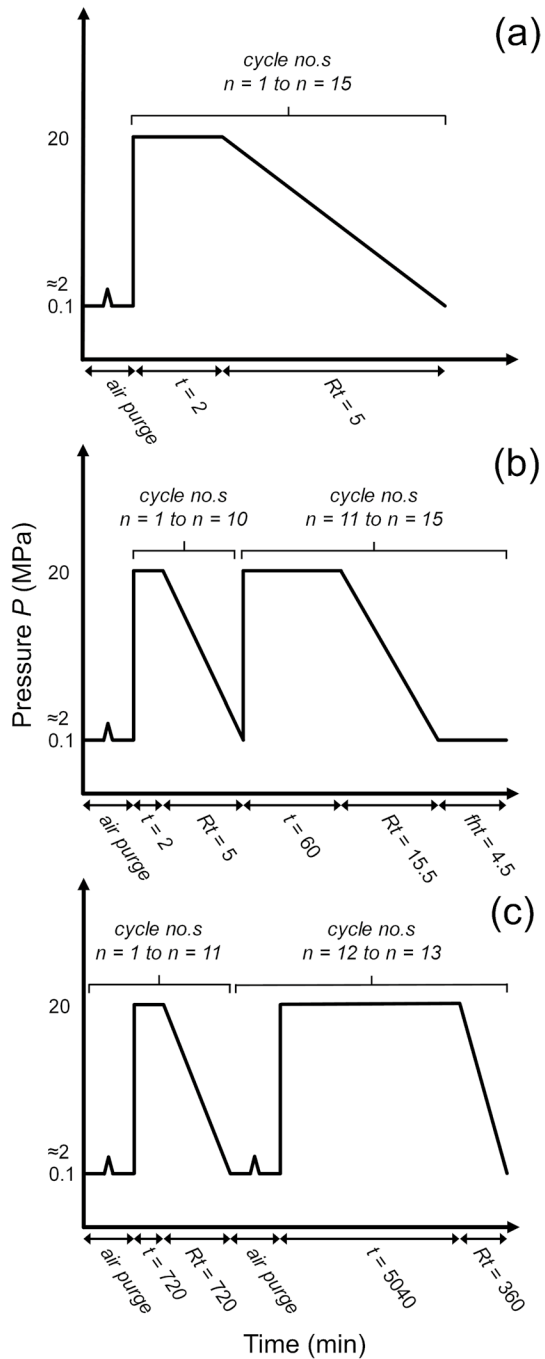
generally involved increasing the main CO_2 treatment chamber pressure from atmospheric to a maximum pressure (P) and holding for a period of time (t) at a constant temperature (T) before being linearly released with respect to a pressure-release-time (Rt) and holding at atmospheric pressure for a final hold time (fht), if required, depending on the treatment regime. Linear pressure venting over time was performed manually using control valves and the liquid CO_2 pump where required. The plant was designed to treat one wood specimen at a time and any released sap could be collected from the bottom of the treatment chamber whenever atmospheric pressure was reached.

The plant design was extended for part of this study to include CO_2 gas drying capability to remove bound, or cell-wall water, after the dewatering of free-water. Drying involved venting liquid CO_2 from the treatment chamber whilst maintaining 20 MPa pressure in the treatment cylinder and was similar to a previously reported design by Brown et al. (2008). The CO_2 regulator outlet pressure and vent rate were controlled at 0.15 MPa and 2 L/min, respectively, by means of a 0–2 bar outlet pressure Swagelok KPR regulator and 0–5 L/min Dwyer airflow rotameter which was calibrated for CO_2. A void-space blank was used in the treatment chamber during drying to maximise water uptake and enhance supercritical CO_2 flow through each specimen cross-section at approximately 9 mm min^{-1}.

Specimen weights and dimensions were recorded (if applicable) before dewatering (green state), after dewatering, after each CO_2 gas drying cycle, and after oven-drying to give initial, dewatered, and CO_2 gas dried MCs.

Dewatering experimental factorial procedure

Experimental supercritical beech dewatering, and drying, was performed on *N. fusca* using three schedules (Table 1), with six replicates per treatment. The first two dewatering schedules (labelled 'radiata' and 'nitens' respectively) were previously optimised for dewatering the free-water from *P. radiata* sapwood (Pearson et al. 2019a), and *E. nitens* heartwood (Pearson et al. 2022). The third schedule (labelled 'beech') was developed based upon anatomical results and fluid dynamics dewatering predictions in this study for dewatering free-water followed by drying bound-water from *N. fusca* heartwood.

The 'radiata' schedule involved cycling the supercritical CO_2 pressure (P) between atmospheric and 20 MPa for a total of 15 pressure cycles as shown in Fig. 3a. The 'nitens' schedule involved repeating the radiata schedule but the pressure hold time (t) and pressure release time (Rt) were both increased, and a *fht* was introduced for the last 5 pressure cycles (Fig. 3b). The 'beech' schedule was initially similar to the 'radiata' and 'nitens' schedules but again with increased pressure hold (t) and Rt, and the exclusion of any *fht* for the first 11 pressure cycles. The t and Rt values were then increased for the last two pressure cycles 12 and 13 when the moisture removal mechanism was switched from free-water dewatering to bound-water drying for the pressure hold period (Fig. 3c).

Table 1 Dewatering and drying factorial design and control variable levels for beech experiments

Variable	No. control variable levels (values)		
	'radiata' schedule	'nitens' schedule	'beech' schedule
Maximum pressure P (MPa)	1 (20)	1 (20)	1 (20)
Temperature T (°C)	1 (50)	1 (50)	1 (50)
Pressure hold time t (min)*	1 (2)	2 (2 [cycles 1–10], 60 [cycles 11–15])	2 (720 [cycles 1–11], 5040 [cycles 12–13])
Pressure release time (Rt) (min)	1 (5)	2 (5 [cycles 1–10], 15.5 [cycles 11–15])	2 (720 [cycles 1–11], 360 [cycles 12–13])**
Final hold time (fht) (min)	NA	2 (0 [cycles 1–10], 4.5 [cycles 11–15])	NA
Maximum No. pressure cycles***	15	15	13
No. replicates	6	6	6
Total No. experiments	6	6	6

NA not applicable; *No.* number; *Also previously called the Initial Pressure Hold Time t_i for the radiata schedule (Pearson et al. 2022); **drying plant-configuration employed; ***refer to schedule charts Fig. 3

The weight and dimensions of all dewatered specimens were recorded immediately after randomised treatment and after oven-drying before being coated in paraffin wax for collapse distortion assessment.

Regression modelling of experimental dewatering data

For the supercritical dewatering and drying results each measurement of MC was scaled to range between zero (fully dewatered), and unity (green) using Eq. 1. The minimum MC for *N. fusca* was assumed to be equal to the experimental limit previously obtained for *P. radiata* (Pearson et al. 2019a), where a *MCmin* of 40.1% represented the mean minimum possible dewatered MC including bound-water.

$$\text{MCsc}_{ijk} = \left(\text{MC}_{ijk} - \text{MC}_{\min} \right) / \left(\text{MC}_{ik} - \text{MC}_{\min} \right) \qquad (1)$$

where MCsc_{ijk} = scaled MC for specimen i after j pressure cycles for schedule k; MC_{ijk} = MC of specimen i after j pressure cycles for schedule k (%); MC_{ij0} = initial (green) MC of specimen i for schedule k (%); $\text{MC}_{\min}$ = the minimum MC (%).

The mean scaled moisture content (MCsc) was calculated for each cycle for each of the three dewatering schedules:

$$\overline{\text{MCsc}_{ik}} = \sum_{j=1}^{n} \text{MSsc}_{ijk} / n \qquad (2)$$

where n is the number of specimens per schedule ($n = 6$ for all schedules).

Ninety-five percent confidence intervals were calculated for each mean under the assumption of normality:

$$\overline{MCsc_{jk}} \pm t \times SD_{jk}/\sqrt{n} \tag{3}$$

where SD is the standard deviation for schedule k at cycle j and t is a t-value with $n-1$ degrees of freedom ($t = 2.571$).

A comparison of *N. fusca* dewatering behaviour was made with *P. radiata* and *E. nitens* using the universal dewatering model developed originally for *P. radiata* (Pearson et al. 2019a) and refitted for *E. nitens* (Pearson et al. 2022). The previously developed *P. radiata* and *E. nitens* models include terms for a number of experimental factors (maximum pressure P, temperature T, initial pressure hold time t_i, and pressure release time Rt) but for the *N. fusca* experiments, these experimental factors were all set to constant values of $P = 20$ MPa, $T = 50$ °C, $t = t_i = 2$ min, $Rt = 5$ min. A reduced version of the model was therefore fitted which excluded terms for these experimental factors to compare *N. fusca*, *E. nitens* and *P. radiata* free-water dewatering from the open hydrofluidic cellular network using the radiata schedule. The model (Eq. 4) is based on the Chapman-Richards (CR) growth curve (Chapman 1961) and includes a slope parameter a, and a shape parameter b. Parameter estimates were obtained by fitting the equation as a nonlinear mixed model using the R *nlme* procedure.

$$MCsc_{ij} = 1 - \left(1 - e^{(-(a+R_i)\times j)}\right)^b + e_{ij} \tag{4}$$

where Ri are random effects for each specimen assumed to be independently and identically distributed (iid) normal variables with zero mean; e_{ij} are error terms assumed to be *iid* normal with zero mean; a and b are fitted model coefficients; $j =$ pressure cycle number ($0 \leq j \leq 10$).

Fundamental CFD modelling of the dewatering process

Free-water dewatering from the open hydrofluidic lumen network was assessed by means of a previously developed two-dimensional (2D) Ansys Fluent computational fluid dynamics (CFD) dewatering model (Pearson et al. 2019a, 2022). The CFD model was based upon the fundamental phenomenon of pressurised CO_2 gas diffusion into an open wood cell lumen, as represented by a sap-filled capillary tube with diameter equivalent to the mean pore size, followed by depressurisation to cause liquid displacement due to gas bubble back-pressure. The theoretical amount of free-water associated with the open hydrofluidic network within the wood was estimated from wood anatomy, MC and mean basic density (Siau 1995; Rijsdijk and Laming 2006). Differences between theoretical and experimental dewatering when represented by an effective CO_2 diffusion coefficient (*Deff*) allowed a lumped-parameter

combined estimate of wood porosity and tortuosity for dewatering characterisation compared to other species (Shen and Chen 2007; Cussler 2014).

Air-drying

One randomly selected specimen from each of the six trees was air-dried from green in a temperature and humidity controlled conditioning environment designed to achieve 12% equilibrium MC (Hailwood and Horrobin 1946). During air-drying, temperature was controlled to 20 ± 0.17 °C, humidity to $65 \pm 0.34\%$ ($\pm 95\%$ C.I. root-mean-squared-error) and the mean airflow across the specimen was measured with a Kestrel 4200 air-flow meter supplied by Nielsen-Kellerman USA, was 3.60 cm/s (SD 0.04 cm/s). Drying was performed until the third mean direction of mass change (ASTM 2014a). MC was calculated through pre- and post-conditioning weights and after oven-drying of the air-dried specimens.

Free-shrinkage

Six randomly selected beech specimens were selected from each tree for solvent drying to obtain free-shrinkage. Each specimen was weighed after volume measurement and immersed in 96% (*w/w*) ethanol. All specimens were held at 21 °C for 7 days before the ethanol solution was replaced. After 25 solution replacements, the specimens were stored in a vacuum chamber with silica gel desiccant at 0.05 MPa and 21 °C before being weighed daily until the maximum percentage change in weight for any specimen was less than 0.25%. After alcohol drying the specimens were re-weighed for MC calculation.

Collapse assessment

Collapse was assessed from changes in the external volume, cross-sectional area, and cross-sectional perimeter. Normalised collapse ratios were calculated for all treated specimens by dividing all measurements by pre-treatment green dimensions. As with
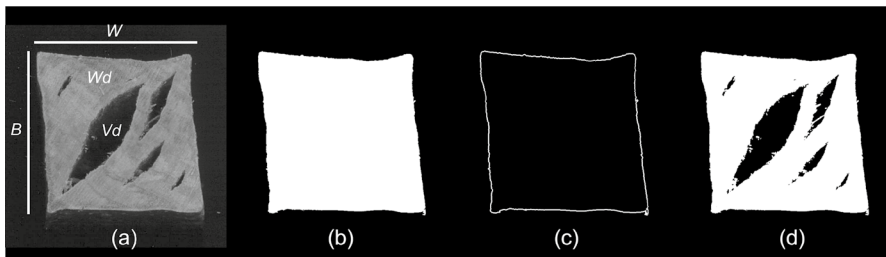
Fig. 4 Representative images for free-shrinkage and collapse measurement. **a** Original cross-section image, of width (*W*) and breadth (*B*), showing areas of wood (*Wd*) compared to void areas (*Vd*). **b** Mask area excluding voids. **c** Perimeter (*P*) length. **d** Void area and wood area mask. Scale: $B = W \approx 25$ mm

the previous study (Pearson et al. 2022), external volumetric specimen collapse was calculated by means of water volume displacement at 21 °C. After volumetric measurement each specimen was cross-cut into two specimens measuring 25 mm (rad)×25 mm (tan)×100 mm (long), and an image taken of one freshly cut face at a resolution of 400 dpi (Fig. 4a). Collapse mask-image analysis was performed using Digital Optics V++software to a resolution of 40 μm. From the images, the total cross-sectional area excluding any collapse voids (Fig. 4b), and total external perimeter length (Fig. 4c) were measured. The total cross-section void collapse area and remaining wood area per specimen cross-section were then calculated by difference from Fig. 4b and d.

Collapse measurements were compared, where applicable, to initial green wood length (L), width (W) and breadth (B) dimensions for each specimen (Eqs. 5–8) Tests of differences in beech collapse distortion between treatments were performed using ANOVA (Analysis of variance) and Tukey's test using the *aov* and *TukeyHSD* procedures in R. The treatments compared beech distortion after oven-drying, air-drying, and treatments with the radiata, nitens and beech schedules. Collapse measurement variables were isolated by subtracting free-shrinkage that was obtained from the ethanol-dried specimens because free-shrinkage is unavoidable when bound-water is removed from wood cell walls (Bodig and Jayne 1982). Relationships between collapse distortion and MC were determined using logistic regressions with quasibinomial distribution fitted using the R *glm* procedure.

$$\text{External Collapse Volume Ratio}_j = V_{ODj} / \left[V_{Gj} \sum_{i=1}^{N=6} \left(\frac{V_{EtOHi}}{V_{Gi}} \right) / N \right] \tag{5}$$

$$\text{Internal Collapse Wood Area Ratio}_j = \frac{A_{Wdj}}{B_{Gi} W_{Gi} \left[\sum_{i=1}^{N=6} \left(\frac{(V_{EtOHi}/L_{EtOHi})}{B_{Gi} W_{Gi}} \right) / N \right]} \tag{6}$$

$$\text{Internal Collapse Void Area Ratio}_j = A_{Vdj} / \left[B_{Gi} W_{Gi} \sum_{i=1}^{N=6} \left(\frac{(V_{EtOHi}/L_{EtOHi})}{B_{Gi} W_{Gi}} \right) / N \right] \tag{7}$$

$$\text{External Collapse Length Ratio}_j = \frac{P_j}{\left(2B_{Gj} + 2W_{Gj} \right) \left[\sum_{i=1}^{N=6} \left(\frac{4\left(\sqrt{V_{EtOHi}/L_{EtOHi}} \right)}{2B_{Gi} + 2W_{Gi}} \right) / N \right]} \tag{8}$$

where V = volume [unit = L^3]; A = area [L^2]; P = perimeter [L]; L = longitudinal specimen length [L]; B = specimen breadth [L]; W = specimen width [L]; OD = oven-dried; Subscripts: $EtOH$ = ethanol-dried; G = green specimen; Wd = wood; Vd = void; i = ith ethanol-dried specimen; j = jth treatment specimen; N = total number of ethanol-dried specimen replicates

Table 2 Mean basic density, green MC and saturation for all *N. fusca* specimens

Tree no.	Basic density (kg/m^3)	Green MC (%)	Saturation (%)
1	497.46 ab	118.31 b	86.81 bc
2	463.61 b	140.72 a	92.44 ab
3	473.20 b	143.57 a	98.06 a
4	521.77 a	101.17 c	79.73 c
5	519.99 a	117.22 bc	91.92 ab
6	476.04 b	143.57 a	98.89 a
Overall mean (pooled SD)	492.01 (24.58)	127.43 (9.70)	91.31 (4.59)

Values in each column followed by the same letter do not differ significantly (Tukey's test, $\alpha = 0.05$)

**Table 3** Anatomical dimensions for 6 specimens of *N. fusca*

log source No.		1	2	3	4	5	6	
Vessels	Area	26.3 ab	33.9 a	31.7 a	22.0 b	25.6 ab	28.8 ab	%
	Mean Area	2052	2399	2250	2022	1743	1823	μm^2
	Mean Diameter	68.2 a	66.3 a	64.7 a	67.7 a	58.1 a	64.3 a	μm
Fibres	Area	15.8 a	8.5 b	17.5 a	17.7 a	15.0 a	18.8 a	%
	Mean Area	60	68	78	61	65	70	μm^2
	Mean Diameter	9.9 b	13.1 ab	11.0 b	9.6 b	10.8 b	11.0 b	μm
Wall thickness	Mean	3.9 b	6.0 a	3.5 b	4.0 b	4.3 b	3.5 b	μm
Tension wood		✓	✓	✗	✗	✓	✓	
Tyloses		✓	✓✓	✗	✗	✗	✓	

Values are average of 5 replicate measurements (5 fields of view). Values in each row followed by the same letter do not differ significantly (Tukey's test, $\alpha = 0.05$)

Results and discussion

Wood quality and anatomy

The mean basic density and green MC for all 36 beech specimens was 492.0 kg/m^3 (SD 24.6 kg/m^3) with a range of 403.1–555.9 kg/m^3, and 127.4% (SD 9.7%) with a range of 86.3–162.1 kg/m^3, respectively. The mean percentage saturation (Ross 2010) was calculated using a mean wood cell wall density of 1.54 g/cm^3 (Siau 1995; Rijsdijk and Laming 2006) and equalled 91.3% (SD 4.6%) with a range of 73.0–99.8%. Significant differences were observed for basic density, green MC and saturation with respect to tree number but not specimen position in tree (Table 2). Basic density and green MC values were comparable with previously reported ranges of 440–590 kg/m^3 (Entrican et al. 1951; Reid 1953; Orman and Harris 1964; Conway 1974; Wardle 1984) and 109–117% (Kininmonth 1964), although *N. fusca* from the Reefton area (including Maruia) was known to be typically less dense than the national average (Reid 1953; Orman
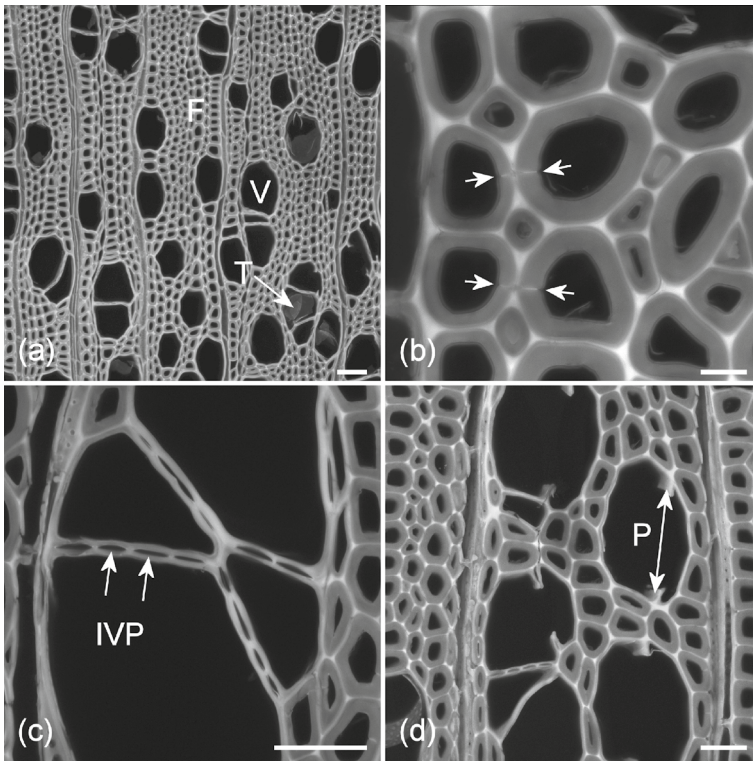
Fig. 5 **a** Red beech confocal autofluorescence of transverse view, excitation 488 nm, emission 500–550 nm, average projection. F = fibre, V = vessel, T = tylosis. Scale bar = 60 μm. **b** Fibre pits, single optical slice. Arrowheads show the fibre pits occluded with extractives. Scale bar = 10 μm. **c** Intervascular pits (IVP, arrows), scale bar = 30 μm. **d** Perforation plate (P, arrow), scale bar = 30 μm. Range of scale is fibre pit 350 nm, IVP 10 μm, perforation plate 65 μm

and Harris 1964). The mean saturation was higher than the national mean of 75% reported by Conway (1974).

Nothofagus fusca has small vessels averaging 64.9 μm (SD 8.8 μm) in diameter and occupying 22–34% (mean 28.0% (SD 0.1%)) of the wood volume. Fibres have a mean lumen diameter of 10.9 μm (SD 0.9 μm) and a mean wall thickness of 4.2 μm (SD 0.5 μm). Variation in cell dimensions among the 6 microscopy specimens is shown in Table 3. Figure 5 shows the general wood anatomy of *N. fusca* with vessels solitary or in small radial groups. Fibres are thick-walled and axial parenchyma is very rare adjacent to growth rings or absent. Tyloses and gelatinous fibres are common. Pits between fibres are sparse and occluded with extractives. No pits between fibres and vessels were observed. Intervascular and vessel to ray pits are large and oppositely arranged (Fig. 5).
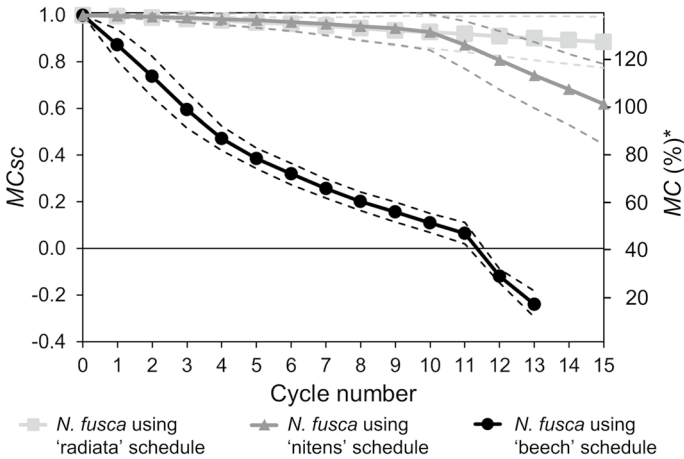
Fig. 6 Mean experimental scaled MC (MCsc) as a function of pressure cycle number for *N. fusca* using 'radiata' (Pearson et al. 2019a), 'nitens' (Pearson et al. 2022) and 'beech' dewatering and drying schedules, respectively. The dotted lines denote 95% confidence intervals. *Calculated using mean green MC calculated from beech schedule treated specimens

Regression modelling

Mean scaled MC (MCsc) and MC of beech at each cycle for each of the three treatment schedules is shown in Fig. 6. Beech treated with the radiata schedule achieved a mean MCsc of 0.92 ± 0.07 (95% CI) after 10 pressure cycles, and 0.88 ± 0.11 after 15 cycles when MCsc reduced by only 0.0078 ± 0.0073 per cycle. Switching to the nitens schedule after cycle 10 resulted in a more significant MCsc reduction of 0.62 ± 0.17 by cycle 15. Over cycles 11–15 of this schedule, MCsc decreased by 0.31 ± 0.15 or 0.062 ± 0.030 per cycle, an eightfold improvement compared with the radiata schedule. The beech schedule achieved a mean MCsc of 0.11 ± 0.04 after 10 cycles, with the MC reducing below the minimum achievable via dewatering of 40.1% (i.e. when MCsc$=0$) by cycle 12. The mean MCsc, after a mechanism switch from dewatering to drying, at cycle 13 was -0.24 ± 0.06 indicating that the MC was well below the fibre saturation point after 13 cycles.

The coefficients of the dewatering model (Eq. 4) fitted to *N. fusca* data treated with the radiata schedule are shown in Table 4 along with the coefficients for the same model fitted for *P. radiata* and *E. nitens* for the same schedule. The models are compared in Fig. 7. The coefficient of determination (R^2) for the *N. fusca*

Table 4 Parameter estimates with standard errors for nonlinear mixed models describing *N.fusca*, *E. nitens* and *P. radiata* dewatering using the radiata treatment schedule (Eq. 4)

Parameter	P. radiata		E. nitens		N. fusca	
	Estimate	SE	Estimate	SE	Estimate	SE
a	0.0175	0.0045	0.550	0.039	0.048	0.004
b	1.463	0.033	1.800	0.170	0.781	0.020
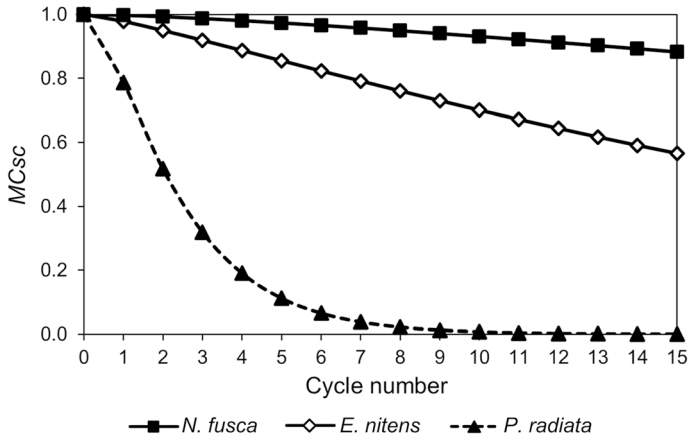
Fig. 7 Scaled MC described by the CR model as a function of pressure cycle number for *N. fusca*, compared to previously reported *E. nitens* (Pearson et al. 2022) and *P. radiata* (Pearson et al. 2019a) treated with the radiata schedule

CR model was 32.3% compared to previously reported R^2 values of 59.0% for *E. nitens* and 84.3% for *P. radiata* (Pearson et al. 2019a, 2022). The relatively lower R^2 for the beech model relates to the fact that variation is unable to be explained for near-zero dewatering. Results show that the radiata schedule was most rapid for *P. radiata* with MCsc being reduced to approximately zero after 10 cycles. The radiata schedule achieved an intermediate result for *E. nitens* with MCsc reduced to 0.70 by 10 cycles. However, dewatering under the radiata schedule was slowest for *N. fusca* with a reduction in MCsc to only 0.93 after 10 cycles. Dewatering was much more rapid for *N. fusca* under the nitens schedule which provided a reduction in scaled MC of 0.265 units over cycles 11 to 15 compared with the radiata schedule which is identical to the nitens schedule up to cycle 10. This was almost identical to the reduction of 0.257 over cycles 11 to 15 for *E. nitens* achieved using the nitens schedule. However, because the initial 10 cycles (radiata schedule) resulted in only a minor reduction in MCsc for *N. fusca*, the scaled MC under the nitens schedule was much higher for *N. fusca* compared with *E. nitens*.

CFD modelling

The mean theoretical amount of free-water contained in the open hydrofluidic (vessel) network of *N. fusca* was calculated to be 56% (dry basis MC). After scaling for vessel moisture dewatering and comparing with the open hydrofluidic CFD capillary model (Pearson et al. 2019a), the dewatered amount of this moisture theoretically reduced by a factor of only 0.02 after 6 pressure cycles (Fig. 7). This meant that the vessels in *N. fusca* heartwood did not exist as an open network (Hass et al. 2010) compared to *P. radiata* sapwood tracheids, or *E. nitens* heartwood vessels, both of which were estimated to have fully dewatered hydrofluidic networks after approximately 6 pressure cycles using the radiata

schedule. Therefore the vessel network of *N. fusca* heartwood had negligible permeability, and calculation of tortuosity as a lumped-parameter based on the effective CO_2 diffusion coefficient (Pearson et al. 2022) was not valid. The modelling and anatomy results confirmed that the vessel network of *N. fusca* heartwood was occluded with tyloses and polyphenol resins even if the network may have been more permeable as sapwood when its specific function was to transport moisture. Based on the CFD modelling and the reported relative ease of drying, *P. radiata* sapwood and *N. fusca* heartwood represent extreme behaviour with *P. radiata* being easy to dewater and dry without distortion, and *N. fusca* being difficult.

Dewatering characterisation for different species

The theoretical extremes for dewatering and drying based on wood anatomy and fundamental CFD modelling provide a useful tool for species characterisation. However, the open hydrofluidic network dewatering behaviour of *N. fusca* yielded conflicting results when comparing theoretical predictions against experimental data and anatomical measurements.

Direct experimental permeability measurements based on Darcy's law may offer a further characterisation variable for prediction of dewatering efficacy (Stamm 1963; Bramhall 1971; Bolton 1988; Hansmann et al. 2002). Expansion of Darcy's law to the Kozeny–Carmen equation also provides the opportunity of incorporating tortuosity and porosity with permeability (Prak 1970; Koponen et al. 1997) and constriction (Berg 2014). However, wood-water relations are complex, and characterisation may require the use of additional variables and assumptions to adequately describe both static and dynamic behaviour. For example, Darcy's law requires laminar flow. Many dimensionless numbers, such as the Bond, Péclet or Reynolds number, require continuous moisture columns which is in contrast with columns that have interspersed gas voids such as Taylor bubbles that occur in the dewatering process (Taylor 1961; Salman et al. 2006).

Dewatering and drying characterisation of the closed-hydrofluidic network of fibres (including occluded vessels) for different hardwood species is also complex and requires both CO_2 and moisture transfer to occur through the cell walls. Wood is highly permeable to supercritical CO_2 (Oberdorfer et al. 2006; Pearson et al. 2022) but moisture transfer across the cell wall requires slower pressure release to avoid rupture (Schneider et al. 2003; Gething et al. 2013). Hence collapse in *N. fusca* was reduced with the beech schedule by means of an increase in depressurisation times (Fig. 3c). An understanding of cell wall porosity (Tremblay et al. 1996; Washusen and Ilic 2001; Chauhan and Walker 2011; Donaldson et al. 2015, 2018) and the relationship between cell wall porosity, tension wood and the fibre saturation point (Hill and Papadopoulos 2001; Almeida and Hernandez 2007; Telkki et al. 2013) may also lead to improved species characterisation and increased accuracy of predictive CFD modelling of the dewatering and drying process.
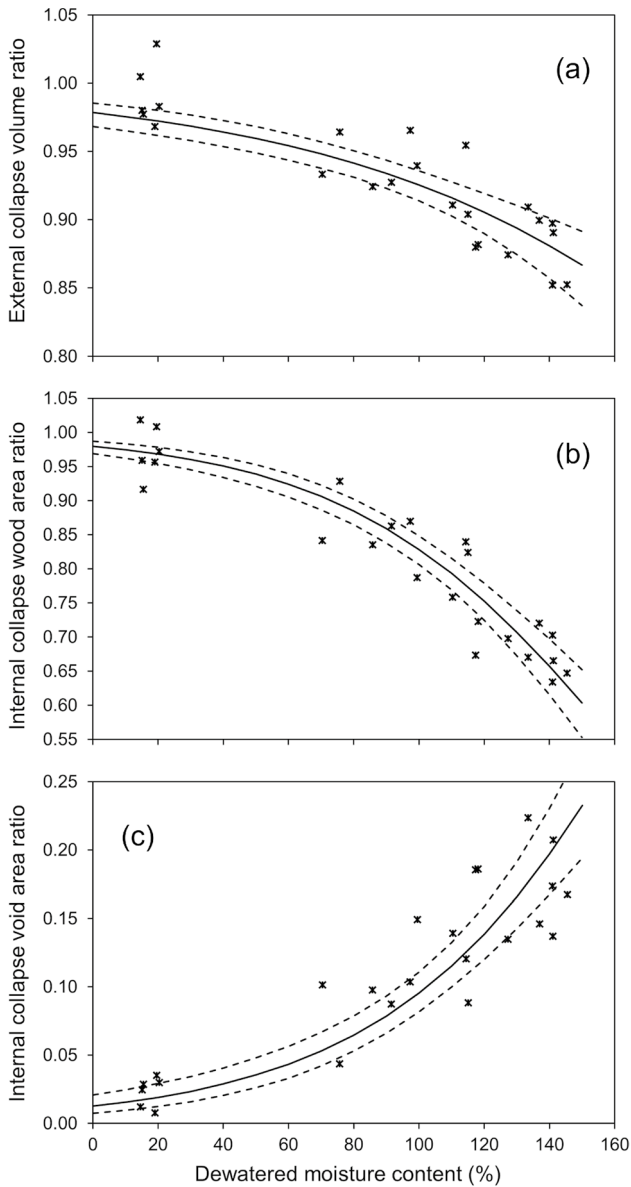
Fig. 8 External volume (**a**), cross-sectional wood area (**b**) and cross-sectional void area (**c**) normalised collapse ratios, compared to pure shrinkage specimen dimensions after oven-drying, as a function of MC prior to oven-drying for all dewatered, oven-dried and air-dried specimens. Solid line shows logistic regression with dashed lines indicating 95% C.I. of the regression curve

Collapse

Collapse distortion of *N. fusca* was found to progressively reduce when treated with the oven-drying, radiata, nitens, beech and air-drying schedules, respectively. The mean volumetric free-shrinkage for the six alcohol-dried specimens was 11.2% (SD 2.2%), with mean central cross-sectional area shrinkage of 11.7% (SD 2.3%) and mean cross-sectional perimeter shrinkage of 6.0% (SD 1.2%). Collapse after oven-drying generally reduced with decreasing initial dewatered MC (Fig. 8). Similar results were found for *E. nitens*, although for a given MC, collapse was higher for *N. fusca* than *E. nitens*. For example, to ensure the mean external volume collapse ratio remains above 0.95, the MC must be less than 67% for *N. fusca* and 82% for *E. nitens*. To achieve the same result for the wood area collapse ratio, the MC must be less than 41% for *N. fusca* and 80% for *E. nitens*. Finally, the internal void area ratio is much higher for *N. fusca* than *E. nitens* at a comparable MC. To ensure the mean void ratio is less than 0.02, the MC must be less than 21% for *N. fusca* and less than 110% for *E. nitens*. Treatment means of collapse distortion ratio variables after compensation for free-shrinkage are shown in Table 5.

The mean external volume of *N. fusca* after treatment with the beech schedule was reduced by 12.0% due to collapse after oven-drying from a green MC of 137.6%, but the volume reduction was only 3.8% after oven-drying from a final mean dewatered MC of 47.0% (Fig. 8a). The volume reduction was further reduced to 2.6% after oven-drying from a final mean dewatered and dried MC of 17.3%. Similarly, the cross-sectional wood area reduced by 33.6, 5.3 and 2.8% when oven-dried from the same MCs of 137.6, 47.0 and 17.3%, respectively. Internal collapse measured by means of the cross-sectional void area ratio also decreased after oven-drying from a green MC of 137.6–18.2% compared to 2.8% when oven-dried from 47.0% MC and 1.7% when oven-dried from 17.3% MC. This meant that a reduction in the dewatered and dried MC of *N. fusca* from green to 17.3% eliminated 77% of oven-dried external volumetric shrinkage and reduced approximately 92% of both internal wood area and internal void collapse (Fig. 8a, b). This compares to collapse reduction in *E. nitens* (Pearson et al. 2022) where the greatest gain (90% reduction) occurred for the external volumetric and internal wood area compared to the internal void area, and shows that *N. fusca* has a different collapse mechanism to *E. nitens*.

Table 5 *Nothofagus fusca* mean moisture content prior to oven-drying, and mean collapse ratios for external volume, cross-sectional wood area and cross-sectional void area by treatment

| N. fusca treatment	MC (%)	Volume ratio	Area ratio	Void area ratio
Oven-dried	125.7 a	0.892 a	0.701 a	0.159 a
Radiata schedule	120.7 a	0.896 a	0.745 a	0.143 a
Nitens schedule	97.1 b	0.942 b	0.836 b	0.113 a
Beech schedule	17.3 c	0.990 c	0.972 c	0.023 b
Air-dried	13.0 c	0.962 bc	0.983 c	0.000 b

Values in each column followed by the same letter do not differ significantly (Tukey's test, $\alpha = 0.05$)

Narrow and radially oriented checks were observed in all *N. fusca* specimens that were treated with the beech dewatering and drying schedule (Fig. 3c). Cross-grain anisotropic checking is another form of distortion that occurs when bulk wood is stressed in tension perpendicular to the longitudinal axis. Compared to collapse, which is primarily caused by water tension forces, checking usually occurs in the radial grain direction due to the larger shrinkage coefficient of wood in the tangential direction, and the orientation of rays which are a structural point of weakness (Kauman 1964a, b; Chafe et al. 1992). Checks can be difficult to separate from collapse, splits and rakes, and are usually assessed by length alone (AS 2000). Checks typically have a negligible cross-sectional void area but they are important because they signify cellular fracture and a corresponding loss of mechanical strength (Bodig and Jayne 1982). Checking can be minimised by optimising the pathway for drying wood to relieve unwanted stresses. However, the stress and strains that cause checking are complex and difficult to measure (Ferrari et al. 2010; Pearson et al. 2015). Collapse, shrinking and checking may occur simultaneously (Dawson and Pearson 2017).

The mean normalised cross-sectional void area of checks for specimens treated with the beech schedule was 0.02 (SD 0.01) (Fig. 9). This low value confirmed that the distortion was more related to checking than other forms of distortion such as collapse. The checks were not quantified further (AS 2000) but previous results
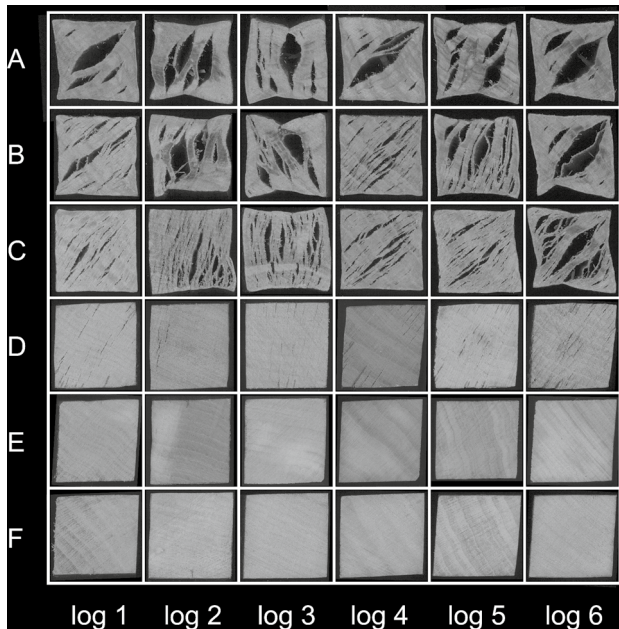
Fig. 9 Middle cross-sections of 25 mm × 25 mm green log-matched red beech specimens after treatment schedules A–F followed by oven-drying. Where treatment schedules A = straight oven-dried control, B = 'radiata' dewatering schedule, C = 'nitens' dewatering schedule, D = 'beech' dewatering and drying schedule, E = air-dried, F = ethanol-dried. Scale: The internal dimensions of each grid square represents a 25 mm × 25 mm section
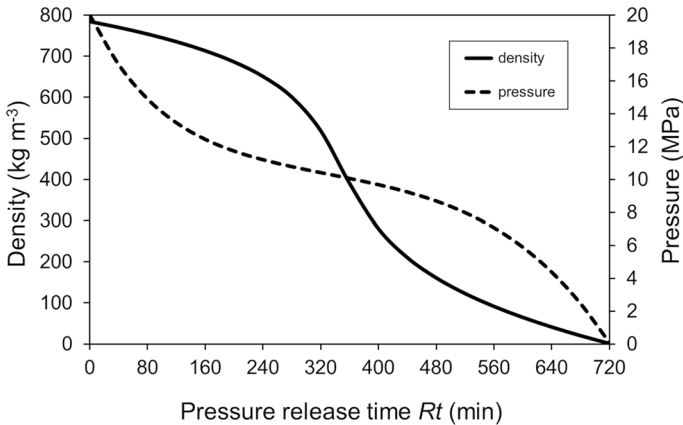
Fig. 10 CO_2 density profile for a linear pressure release from 20 to 0.1 MPa compared to the CO_2 pressure profile for a linear density release from 784.39 to 1.64 kg/m³, for a pressure release time (Rt) of 720 min

confirmed that out of 22 different species, *N. fusca* exhibited the greatest amount of checking after dewatering followed by oven-drying (Dawson and Pearson 2017). A supplementary test revealed that minor checking occurred midway through the pressure release procedure (Rt) (Fig. 3c) for earlier cycle numbers up to about cycle 3, when specimen moisture was at its highest. A plot of CO_2 density as function of pressure release time for the constant (linear) pressure release rate is shown in Fig. 10 and reveals that the greatest CO_2 density change occurred in the middle of the pressure release procedure. Therefore, it was likely that the checking was a form of cell rupture from excessive localised pressure and/or density differences which were exacerbated during later oven-drying. The issue may be ameliorated by further slowing the pressure release rate for earlier pressure cycles or switching to linear density-based depressurisation in the middle of the depressurisation procedure, to reduce elevated pressure or density change differentials (Fig. 10).

Air-drying produced the least collapse but took 6 months for moisture conditioning to complete compared to 18 days (11 days for dewatering and 7 days for drying) for specimens treated with the beech schedule. However, the pressure hold times for cycles 1–11 of the beech schedule were extended to 12 h primarily to reduce the reliance on manual labour during night-time plant operation. Therefore, the overall beech schedule time could be significantly reduced.

Supercritical drying below the fibre saturation point (FSP)

Nothofagus fusca was successfully dried to a minimum mean MC of 17.3% (SD 2.4%) (range 14.5–20.3%) using the water absorption properties of supercritical CO_2. This was well below the FSP estimate of 29% (Forest Products Laboratory 2010) calculated using the Hailwood and Horrobin (1946) model (Thybring and Fredriksson 2023). The mutual absorptions of CO_2 and water are non-ideal in behaviour (King et al. 1992), and the amount of moisture that can be absorbed by

CO_2 at 20 MPa and 50 °C is relatively small at approximately 4 mg/g (Sabirzyanov et al. 2002). Therefore, a sufficient time per pressure cycle of 5040 min was required for adequate drying to occur in cycles 12 and 13 of the beech schedule.

It is not known if the checks associated with the beech schedule specimens would have still been present if they were eliminated from the early dewatering cycles. This is because wood distortion during shrinkage below the FSP can be associated with pre-existing fracture points, but CO_2 is known to create wood softening which may adjust manifest strains such as creep and mechanosorption to reduce distortion (Pearson et al. 2015). Further study on the relationship between CO_2 drying and check formation in *N. fusca* is recommended, including the use of co-solvents to increase the drying rate.

Conclusion

Collapse of *N. fusca* heartwood can be significantly reduced when dewatered and dried using supercritical CO_2 with a specifically designed schedule. Results have shown that when compared to oven-drying, collapse can be reduced by 92% for both normalised internal wood area and internal void area collapse, and 77% for normalised external volumetric shrinkage collapse.

Anatomical measurements confirmed that the heartwood of *N. fusca* generally contains tension wood and is occluded with tyloses and polyphenol resins. This means that *N. fusca* does not dewater easily because its open hydrofluidic network is compromised and moisture expelled by means of supercritical CO_2 needs to pass through restricted hydrofluidic pathways and cell walls. This behaviour was confirmed by treating *N. fusca* with dewatering schedules that were previously optimised for *P. radiata* and *E. nitens*, and by using a previously developed CFD model to predict dewatering only from the open hydrofluidic cellular network. Based on these results a dewatering schedule was developed specifically for beech using greater CO_2 and moisture diffusion time. The schedule was extended to incorporate drying and resulted in a reduction in MC of *N. fusca* to well below the FSP.

The beech specimens took 18 days to reach 17.3% MC, using the dewatering and drying schedule, but displayed some checking from depressurisation during initial dewatering pressure cycling. In contrast, air-dried control specimens showed no collapse or checking but took 6 months to reach 12% MC.

The supercritical CO_2 dewatering and drying process has been successfully demonstrated on *N. fusca*, which is a species at the extreme end of those that are difficult to dry without causing unwanted distortion. Supercritical CO_2 dewatering and drying could include co-solvents and be combined with extractives separation, preservative treatment, and mechanical forming of wood in one plant to make a potentially economically viable process with an improved energy, environmental and carbon footprint. The removal of extractives during dewatering and drying using co-solvents may also improve permeability in *N. fusca* and therefore reduce overall treatment time. The supercritical process has an estimated higher capital cost but doesn't require energy for moisture evaporation and captures all volatiles compared to conventional kiln-drying. A techno-economic analysis is suggested to compare

supercritical dewatering unit operation scenarios along with further studies to test for the effect of specimen size and ways to eliminate checking.

Author contributions All authors contributed to writing and reviewing the manuscript.

Declarations

Conflict of interest The authors declare that they have no conflict of interest.

References

Aggarwal S, Johnson S, Hakovirta M, Sastri B, Banerjee S (2019) Removal of water and extractives from softwood with supercritical carbon dioxide. Ind Eng Chem Res 58:3170–3174

Almeida G, Hernandez RE (2007) Influence of the pore structure of wood on moisture desorption at high relative humidities. Wood Mater Sci Eng 2:33–44

AS (2000). Australian Standard 2082–2000 Timber—Hardwood—Visually stress-graded for structural purposes. Standards Australia.

Asafu-Adjaye O, Via B, Sastri B, Banerjee S (2021) Mechanism of dewatering porous structures with supercritical carbon dioxide. Case Stud Chem Environ Eng, 4.

ASTM (2014a) Standard guide for moisture conditioning of wood and wood-based materials. ASTM Vol. 04.10 Wood. D4933-99 (Reapproved 2010).

ASTM (2014b) Standard test methods for small clear specimens of timber. ASTM Vol. 04.10 Wood. D143-14.

ASTM (2014c) Standard test methods for specific gravity of wood and wood-based materials. ASTM Vol. 04.10 Wood. D2395-07a.

Berg CF (2014) Permeability description by characteristic length, tortuosity, constriction and porosity. Transp Porous Med 103:381–400

Blakemore P, Northway R (2009) Review of, and recommendations for, research into preventing or ameliorating drying related internal and surface checking in commercially important hardwood species in south-eastern Australia. Forest and Wood Products Australia (FWPA). Level 4, 10–16 Queen street, Melbourne, Victoria, Australia. Project No. PNB047–0809. pp 84.

Bodig J, Jayne BA (1982) Mechanics of wood and wood composites. Van Nostrand Reinhold Australia Pty. Ltd. Australia. pp 712.

Bolton AJ (1988) A re-examination of some deviations from Darcy's Law in coniferous wood. Wood Sci Technol 22:311–322

Bramhall G (1971) The validity of Darcy's law in the axial penetration of wood. Wood Sci Technol 5:121–134

Brown ZK, Fryer PJ, Norton IT, Bakalis S, Bridson RH (2008) Drying of foods using supercritical carbon dioxide—investigations with carrot. Innov Food Sci Emerg Technol 9:280–289

Bulushi KA, Attard TM, North M, Hunt AJ (2018) Optimisation and economic evaluation of the supercritical carbon dioxide extraction of waxes fromwaste date palm (*Phoenix dactylifera*) leaves. J Cleaner Prod 186:988–996

Chafe SC, Barnacle JE, Hunter AJ, Ilic J, Northway R, Rozsa AN (1992) Collapse: an introduction. CSIRO Division of Forest Products, Melbourne, Australia. pp 13.

Chapman DG (1961) Statistical problems in population dynamics. In: Proceedings of the 4thberkeley symposium on mathematical statistics and probability, vol 4. University ofCalifornia Press, Berkeley, USA, pp 153–186

Chauhan SS, Walker JCF (2011) Wood quality in artificially inclined 1-year-old trees of *Eucalyptus regnans*—differences in tension wood and opposite wood properties. Can J for Res 41:930–937

Clifton NC (1990) New Zealand timbers. GP Print Ltd. New Zealand, pp 170.

Conway MJ (1974) Timber properties and uses of the New Zealand beeches. New Zealand Forest Service. Wellington, New Zealand, pp 43.

Cussler EL (2014) Diffusion mass transfer in fluid systems, 3rd edn. Cambridge University Press, University Printing House, Cambridge, p 631

Dawson BSW, Pearson H (2017) Effect of supercritical CO_2 dewatering followed by oven-drying of softwood and hardwood timbers. Wood Sci Technol 51:771–784

Dawson BSW, Pearson H, Kroese H, Sargent R (2015) Effect of specimen dimension and pre-heating temperature on supercritical CO_2 dewatering of radiata pine sapwood. Holzforschung 69:421–430

Donaldson LA, Kroese H, Hill SJ, Franich RA (2015) Detection of wood cell wall porosity using small carbohydrate molecules and confocal fluorescence microscopy. J R Microsc Soc 259:228–236

Donaldson LA, Cairns M, Hill SJ (2018) Comparison of micropore distribution in cell walls of softwood and hardwood xylem. Plant Physiol 178:1142–1153

Entrican AR, Ward WC, Reid JS (1951) The physical and mechanical properties of the principal indigenous woods of New Zealand. New Zealand Forest Service. Wellington. New Zealand, pp 83

Fernandes J, Kjellow AW, Henriksen O (2012) Modelling and optimization of the supercritical wood impregnation process—focus on pressure and temperature. J Supercrit Fluids 66:307–314

Ferrari S, Pearson H, Allegretti O, Gabbitas B (2010) Measurement of internal stress in radiata pine sapwood during drying using an improved online sensor. Holzforschung 64:781–789

Forest Products Laboratory (2010) Wood handbook-Wood as an engineering material. General Technical Report FPL-GTR-190. Department of Agriculture, Forest Service, Forest Products Laboratory. Madison, pp 508.

Franich RA, Gallagher S, Kroese H (2014) Dewatering green sapwood using carbon dioxide cycled between supercritical fluid and gas phase. J Supercrit Fluids 89:113–118

Gabitov RF, Khairutdinov VF, Gumerov FM, Gabitov FR, Zaripov ZI, Gaifullina R, Farakhov MI (2017) Drying and impregnation of wood with propiconazole using supercritical carbon dioxide. Russ J Phys Chem B 11:1223–1230

Gething BA (2011) The computational modeling of supercritical carbon dioxide flow in solid wood material. The Pennsylvania State University, PhD, p 277

Gething BA, Janowiak JJ, Morrell JJ (2013) Using computational modeling to enhance the understanding of the flow of supercritical carbon dioxide in wood materials. J Supercrit Fluids 82:27–33

Hailwood AJ, Horrobin S (1946) Absorption of water by polymers: analysis in terms of a simple model. Trans Faraday Soc 42B:84–102

Hansmann C, Gindl W, Teischinger A, Wimmer R (2002) Permeability of wood—a review. Drevarsky Vyskum/Wood Res 47:1–16

Haslett AN, Kininmonth JA (1986) Pretreatments to hasten the drying of *Nothofagus fusca*. N Z J For Sci 16:237–246

Hass P, Wittel FK, McDonald SA, Marone F, Stampanoni M, Herrmann HJ, Niemz P (2010) Pore space analysis of beech wood: the vessel network. Holzforschung 64:639–644

Hay JN, Johns K (2000) Supercritical fluids—a potential revolution in wood treatment and coating. Surf Coat Int 3:106–110

Herrero M, Cifuentes A, Ibañez E (2006) Sub- and supercritical fluid extraction of functional ingredients from different natural sources: plants, food-by-products, algae and microalgae. A review. Food Chem 98:136–148

Herritsch A, Nijdam JJ (2012) A computational tool to investigate different drying methods for New Zealand indigenous red beech timber (*Nothofagus fusca*). Asia-Pac J Chem Eng 7:555–562

Herritsch A, Dronfield J, Nijdam JJ (2010) Intermittent and continuous drying of red beech timber from the green condition. Drying technol 28:269–277

Hill C, Papadopoulos AN (2001) A review of methods used to determine the size of the cell wall microvoids of wood. J Inst Wood Sci 15:337–345

Hillis WE, Inoue T (1967) The polyphenols of *Nothofagus* species—II.: the heartwood of *Nothofagus fusca*. Phytochemistry 6:59–67

Hillis WE, Orman HR (1962) The extractives of New Zealand *Nothofagus* species. J Linn Soc (Bot) 58:175–185

Jones TG, Walker JCF (1999) Decompression drying of *Pinus radiata* sapwood chips. For Prod J 49:67–72

Kauman WG (1964a) Cell collapse in wood (Part I). Holz Roh-Werkst 22:183–196

Kauman WG (1964b) Cell collapse in wood (Part II). Holz Roh- Werkst 22:465–472

Kaye B, Cole-Hamilton DJ, Morphet K (1999) Supercritical drying: a new method for conserving waterlogged archaeological materials. Stud Conserv 45:233–252

Khalloufi S, Almeida-Rivera C, Bongers P (2010) Supercritical-CO_2 drying of foodstuffs in packed beds: experimental validation of a mathematical model and sensitive analysis. J Food Eng 96:141–150

King MB, Mubarak A, Kim JD, Bott TR (1992) The mutual solubilities of water with supercritical and liquid carbon dioxides. J Supercrit Fluids 5:296–302

Kininmonth JA (1971) Effect of steaming on the fine structure of *Nothofagus fusca*. N Z J For Sci 1:129–139

Kininmonth JA (1972) Permeability and fine structure of certain hardwoods and effects on drying. II. Differences in fine structure of *Nothofagus fusca* sapwood and heartwood. Holzforschung 26:32–38

Kininmonth JA (1964) Seasoning of beech timbers. In: Beech Forestry in New Zealand. Symposium held at the Forest Research Institute Rotorua, 28–31 July, 1964. pp 15–23

Kjellow AW, Henriksen O (2009) Supercritical wood impregnation. J Supercrit Fluids 50:297–304

Kopcak U, Mohamed RS (2005) Caffeine solubility in supercritical carbon dioxide/co-solvent mixtures. J Supercrit Fluids 34:209–214

Koponen A, Kataja M, Timonen J (1997) Permeability and effective porosity of porous media. Phys Rev E 56:3319–3325

Langrish TAG, Keey R, Kumar M (1992) Improving the quality of timber from red beech (*N. fusca*) by intermittent drying. Drying Technol 10:947–960

Liu H, Xie J, Zhang J (2022) Moisture transfer and drying stress of *Eucalyptus* wood during supercritical CO_2 (ScCO_2) dewatering and ScCO_2 combined oven drying. BioResources 17:5116–5128

Lloyd J (1976) Extractives of New Zealand Nothofagus species. 3. Extractives of red beech heartwood, sapwood and bark. WC Wood Materials and Biotechnology. Publication Type:13 Division Report. Series Number:7. pp 20.

Matsunaga M, Kataoka Y, Matsunaga H, Matsui H (2010) A novel method of acetylation of wood using supercritical carbon dioxide. J Wood Sci 56:293–298

Oberdorfer G, Leichti RJ, Morrell JJ (2006) Internal pressure development and deformation during supercritical fluid impregnation of selected wood-based materials. Wood Fiber Sci 38:190–205

Orman HR, Harris JM (1964) Properties of beech timbers. In: Beech Forestry in New Zealand. Symposium held at the Forest Research Institute Rotorua, 28–31 July, 1964. pp 9–14.

Pearson H, Ormarsson S, Gabbitas B (2015) Nonlinear tensile creep behavior of radiata pine at elevated temperatures and different moisture contents. Holzforschung 69:915–923

Pearson H, Dawson B, Kimberley M, Davy B (2019a) Modelling and optimisation of ceramic and wood dewatering using supercritical CO_2. J Supercrit Fluids 146:15–22

Pearson H, Dawson B, Kimberley M, Davy B (2019b) Predictive modelling of supercritical CO_2 dewatering of capillary tubes. J Supercrit Fluids 143:198–204

Pearson H, Donaldson L, Kimberley M (2022) Mitigation of cellular collapse during drying of Eucalyptus nitens wood using supercritical CO_2 dewatering. IAWA 44:1–20

Prak AL (1970) Unsteady-state gas permeability of wood. Wood Sci Technol 4:50–69

Purnell EVJ (1964) The proportion of heartwood in rimu and beech logs in the Reefton district. In: Beech Forestry in New Zealand. Symposium held at the Forest Research Institute Rotorua, 28–31 July, 1964, p 40.

Reid JS (1953) Beech timbers: Properties and uses of Nothofagus species. New Zealand Forest Service. Wellington. New Zealand. Information Seriers No. 17. pp 40

Rijsdijk JF, Laming PB (2006) Physical and related properties of 145 timbers. Kluwer academic publishers, London, UK, p 380

Sabirzyanov AN, Il'in AP, Akhunov AR, Gumerov FM (2002) Solubility of water in supercritical carbon dioxide. High Temp 40:203–206

Salman W, Gavriilidis A, Angeli P (2006) On the formation of Taylor bubbles in small tubes. Chem Eng Sci 61:6653–6666

Schneider PF, Levien KL, Morrell JJ (2003) Internal pressure measurement techniques and pressure response in wood during treating processes. Wood Fiber Sci 35:282–292

Shen L, Chen Z (2007) Critical review of the impact of tortuosity on diffusion. Chem Eng Sci 62:3748–3755

Siau JF (1995) Wood: Influence of moisture on physical properties. Virginia Polytechnic Institute and State University, Department of Wood Science and Forest Products

Smale M, Bergin D, Steward G (2012) The New Zealand beeches. Establishment, growth and management. New Zealand Indigenous Tree Bulletin No.6. Scion, Rotorua, New Zealand

Stahl M, Bentz M (2004) High-pressure treatment of wood—combination of mechanical and thermal drying in the "I/D Process." Chem Eng Technol 27:1216–1221

Stamm AJ (1963) Permeability of wood to fluids. For Prod J 13:503–507

Taylor GI (1961) Deposition of a viscous fluid on the wall of a tube. J Fluid Mech 10:161–165

Telkki V, Yliniemi M, Jokisaari J (2013) Moisture in softwoods: fiber saturation point, hydroxyl site content, and the amount of micropores as determined from NMR relaxation time distributions. Holzforschung 67:291–300

Thybring EE, Fredriksson M (2023) Wood and moisture. In: Niemz P, Teischinger, Sandberg D (eds) Springer Handbook of Wood Science and Technology.Springer, Cham, 355–397.

Tremblay C, Cloutier A, Fortin Y (1996) Moisture content-water relationship of red pine sapwood above the fiber saturation point and the determination of the effective pore size contribution. Wood Sci Technol 30:361–371

Wardle JA (1984) The New Zealand beeches: ecology utilisation and management. The Caxton Press, New Zealand Forest Service, p 447

Washusen R, Ilic J (2001) Relationship between transverse shrinkage and tension wood from three provenances of *Eucalyptus globulus* Labill. Holz Roh- Werkst 59:85–93

Williams JR, Clifford AA, Al-Saidi SHR (2002) Supercritical fluids and their applications in biotechnology and related areas. Mol Biotechnol 22:263–284

Zhang Z (2000) Identification and evaluation of improved drying methods of new zealand beeches by means of an energy-efficient kiln process. Department of Chemical and Process Engineering, University of Canterbury, Christchurch, New Zealand, p 205

Zhang J, Yang L, Liu H (2021) Green and efficient processing of wood with supercritical CO_2: a review. Appl Sci (switzerland) 11:1–16